

[strongly recommended: read Wilson1975 !]

1. General RG ideas

[Wilson1975, p.777]

Renormalization group theory is technically more demanding than the theory of derivatives or Feynman diagrams. However, most of the unsolved problems in physics and theoretical chemistry are of the kind the renormalization group is intended to solve (other kinds of problems usually do not remain unsolved for long). It is likely that there will be a vast extension of the renormalization group over the next decade as the methods become more clever and powerful; there are very few areas in either elementary particle physics, solid state physics, or theoretical chemistry that are permanently immune to this infection.

[Wilson1975, p.776]

The fourth aspect of renormalization group theory is the construction of nondiagrammatic renormalization group transformations, which are then solved numerically, usually using a digital computer. This is the most exciting aspect of the renormalization group, the part of the theory that makes it possible to solve problems which are unreachable by Feynman diagrams. The Kondo problem has been solved by a nondiagrammatic computer method. The renormal-

[Wilson1975, p.778]

The renormalization group approach is designed to handle fluctuations over many wavelengths. The renormalization group strategy is to divide the full range of wavelengths into subranges of manageable proportions and consider each subrange in sequence. For example, one can consider separately the ranges of wavelengths 1–2 Å, 2–4 Å, 4–8 Å, etc.

Fundamental RG concepts:

- Importance of energy scale separation:
 - Goal: resolve splittings at smallest scales! [Wilson1975, p. 812]
- Logarithmic discretization: interpretation -- energy space vs. real space [Krishna-murthy1980a, p.1007]
- RG transformation: [Wilson1975, p. 816]
 - integrate out high energies, get renormalized H
 - truncate
 - rescale
- Fixed points
 - general idea
 - Kondo model fixed points: - local moment
- strong coupling
 - even/odd iterations [Wilson1975, p. 820]
- RG flow - railroad tracks [Wilson1975, p. 809]
- Deviations from fixed point [Wilson1975, p. 820]



Why logarithmic discretization?

The occurrence of $\int d\varepsilon \frac{1}{\varepsilon}$ terms in perturbation theory indicates that 'all energy scales are equally important' (there is no characteristic energy scale which dominates).

$$\int_E^{2E} d\varepsilon \frac{1}{\varepsilon} = \ln \frac{2E}{E} = \ln 2, \text{ independent of } E \quad ! \text{ [Wilson1975, p. 774]} \quad (1)$$

So, we must collect contributions from all scales, no matter how small!

Logarithmic discretization achieves that: all intervals $I_n = [\Lambda^{-(n+1)}, \Lambda^{-n}]$ make similar contributions:

$$\int_{I_n} d\varepsilon \frac{1}{\varepsilon} = \int_{\Lambda^{-(n+1)}}^{\Lambda^{-n}} d\varepsilon \frac{1}{\varepsilon} = \ln \frac{\Lambda^{-n}}{\Lambda^{-(n+1)}} = \ln \Lambda \quad (2)$$

Why integrate from high to low energies? [Wilson1975, p. 812]

Consider a general Hamiltonian of the hierarchical form

$$H = H_1 + H_2 + H_3 + \dots \quad (3)$$

with

$$\|H_1\| \gg \|H_2\| \gg \|H_3\| \dots$$

Then one should not diagonalize all terms 'at the same time', but instead first, H_1 , then H_2 , then H_3 ...

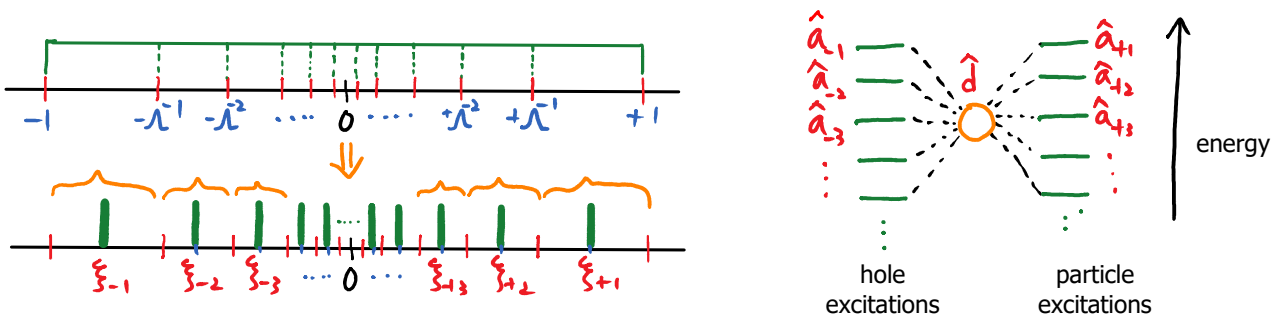
Reason: suppose we have only 95% accuracy for each step, and suppose $\|H_1\| \sim 1, \|H_2\| \sim 0.01$

If we first diagonalize H_1 , then we can compute matrix elements $\langle \alpha | H_2 | \beta \rangle$ with error 0.05 hence with an absolute error of 0.0005, so energy splittings due to H_2 are known with error 5% (0.05 times smaller than $\|H_2\|$). By contrast, if we diagonalize $H_1 + H_2$ together, their levels are known with an accuracy of 0.05. Thus the error would 500% (5 times larger than $\|H_2\|$).

Moral: always treat high energies before low energies!

Why map 'star geometry' to 'chain geometry' ?

Star geometry:



Chain geometry:



The coupling of each interval I_n^\pm with impurity 'renormalizes' it, as described by unitary transformation from old to new basis,

$$|\beta\rangle_{l+1} = |\sigma_{l+1}\rangle |\alpha\rangle_l A^{\alpha\beta}_{l+1}$$

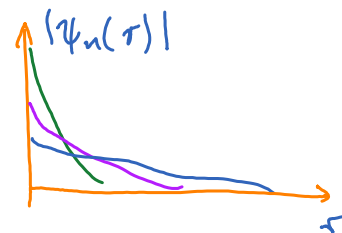
In star geometry, every new site couples to original impurity site, requiring $\langle \beta | \hat{d}_s^\dagger | \beta \rangle_{l+1}$ to be evaluated. Errors accumulate: inaccuracies of early iteration affect impurity-bath coupling at later iterations (because impurity itself is renormalized at each step).

In chain geometry, by contrast, every new site couples only to previous site, and these site-to-site couplings can be computed very accurately (since star-to-chain mapping is a single-particle problem).

What is nature of basis states in star and chain geometries? [Krishna-murthy1980a, p. 1007]

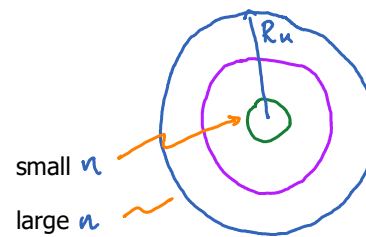
In star geometry, each $\hat{a}_{\pm n}^\dagger$ state is localized in energy around $\epsilon_{\pm n}$, with energy spread $\Lambda^{-n}(1-\Lambda^{-1})$. In real space, corresponding wavefunction $\psi_n(r)$ is peaked at $r=0$, with radial extent

$$R_n \sim \int dr |\psi_n(r)|^2 \sim 1/(\text{energy spread}) \sim \Lambda^n(1-\Lambda^{-1})$$



In chain geometry, each f_n^\dagger state has energy $\epsilon_n \approx 0$, with energy spread $\Lambda^{-n/2}$, and spatial extent $\Lambda^{n/2}$.

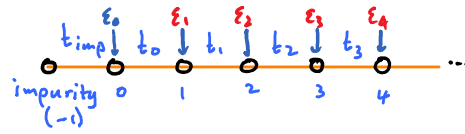
↑
off-diagonal elements of chain Hamiltonian



2. NRG iteration scheme from RG perspective

NRG-II.2

[Wilson1975, Sec VIII]; [Krishna-murthy1980a, Sec. III]



Wilson chain of length N has Hamiltonian

$$\hat{H}^L = H_{loc}(\hat{d}_s, \hat{d}_s^\dagger) + \sum_s t_{imp} \hat{S}_d \cdot \hat{f}_{0s}^\dagger \hat{S}_{ss'} \hat{f}_{0s'} + \sum_{l=0}^{L-1} \sum_s t_l (\hat{f}_{ls}^\dagger \hat{f}_{l+1s} - h.c.) \quad (1)$$

Define $t_l = \Lambda^{-l/2} \tilde{t}_l$, then for large l we have: $\tilde{t}_l \rightarrow \frac{1}{2}(1 + \Lambda^{-1}) = \mathcal{O}(1)$ (NRG-I.3.18) (2)

Therefore, lowest energy splitting of \hat{H}_L is $\mathcal{O}(\Lambda^{-(L-1)/2})$. (3)
coupling between sites $L-1$ and L

To iteratively resolve this splitting, define a sequence of rescaled Hamiltonians:

$$\tilde{H}^L = \Lambda^{(L-1)/2} (\hat{H}^L - E_g^L) \quad (4)$$

chosen to make true ground state energy of equal to zero

then lowest energy splittings in spectrum of \tilde{H}^L are $\mathcal{O}(1)$. [Henceforth tildes indicate rescaled quantities.]

Eq. (4) implies a recursion relation:

$$\tilde{H}^{L+1} = \Lambda^{L/2} (\hat{H}^{L+1} - E_g^{L+1}) \quad (5)$$

$$= \Lambda^{L/2} (\hat{H}^L - E_g^L) + \underbrace{\Lambda^{L/2} t_L}_{= \tilde{t}_L} \sum_s (\hat{f}_{Ls}^\dagger \hat{f}_{L+1s} + h.c.) - \underbrace{\Lambda^{L/2} (E_g^{L+1} - E_g^L)}_{= \delta E_g^{L+1}} \quad (6)$$

$$\tilde{H}^{L+1} = \underbrace{\Lambda^{1/2} \tilde{H}^L}_{\text{rescale}} + \underbrace{\sum_s \tilde{t}_L (\hat{f}_{Ls}^\dagger \hat{f}_{L+1s} + h.c.)}_{\text{enlarge system}} - \underbrace{\delta E_g^{L+1}}_{\text{set ground-state energy to zero}} \quad (7)$$

Symbolic notation:

$$\tilde{H}^{L+1} = \mathcal{T}[\tilde{H}^L] \quad (8)$$

↑ denotes RG-transformation (7)

Question: what happens under repeated applications of \mathcal{T} ? Answer: system flows to a fixed point!

Fixed point Hamiltonian satisfies $\mathcal{T}[\tilde{H}^*] = \tilde{H}^* \quad (9)$

More precisely: for Wilson chains, \mathcal{T} does not have fixed points, but \mathcal{T}^2 (two RG steps) does:

$$\mathcal{T}^2[\tilde{H}^*] = \tilde{H}^* \quad (10)$$

in the sense that the eigenspectrum of \tilde{H}^* and matrix elements of \hat{f}_L remain invariant.

3. Uncoupled bath Hamiltonian: fixed points

NRG-II.3

Key insight by Wilson: fixed points of H_{Kondo} and H_{SIAM} can be understood in terms of the fixed points of the free(!)-electron Hamiltonian,

$$\tilde{H}_0^N = \sum_{l=0}^{L-1} \sum_S \Lambda^{(L-1-l)/2} \tilde{t}_l (f_{ls}^\dagger f_{l+1s} + h.c.) \quad (1)$$

The eigenvalues of \tilde{H}_0^L can be found by diagonalizing a $(L-1) \times (L-1)$ -dimensional matrix, with non-zero matrix elements only just above and below the diagonal:

$$(\tilde{H}_0^L)_{l,l+1} = (\tilde{H}_0^L)_{l-1,l} = \Lambda^{(L-1-l)/2} \tilde{t}_l \quad (2)$$

Particle-hole symmetry implies that eigenvalues come in degenerate pairs, $\pm \eta$. They are given by

$$\text{For } L+1 = \begin{cases} \text{even:} & \pm \eta_j - j = 1, 2, 3, \dots, \frac{1}{2}(L+1) \\ \text{odd:} & \tilde{\eta}_0 = 0, \pm \tilde{\eta}_j - j = 1, 2, 3, \dots, \frac{1}{2}L \end{cases} \quad (3)$$

As L increases, they approach limiting values:

$$\text{For } L+1 = \begin{cases} \text{even:} & \eta_j \xrightarrow{\text{large } L} \eta_j^* \approx \Lambda^{j-1} \\ \text{odd:} & \tilde{\eta}_j \xrightarrow{\text{large } L} \tilde{\eta}_j^* \approx \Lambda^{j-1/2} \end{cases} \quad (4)$$

Not surprising, since \tilde{H}_0^N is rescaled version of a discretized Hamiltonian with diagonal elements

$$\xi_{\pm l} \approx \pm \Lambda^{-l}. \text{ Concretely, for } \Lambda = 2.5, \text{ the fixed-point values are: [Krishna-murthy1980a]}$$

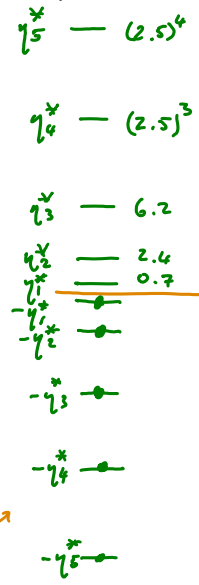
$$\eta_j^*: 0.746856, 2.493206, 6.249995, (2.5)^3, (2.5)^4, \dots, (2.5)^{j-1}, \dots, (N+1) \text{ even}; \quad (3.4)$$

$$\tilde{\eta}_j^*: 1.520483, 3.952550, 9.882118, (2.5)^{7/2}, (2.5)^{9/2}, \dots, (2.5)^{j-1/2}, \dots, (N+1) \text{ odd}; \quad (3.5)$$

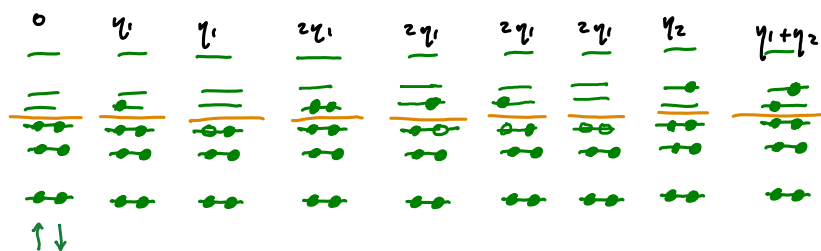
Spectrum for $L+1 = \text{even}$

$$\text{Diagonalized form of } \tilde{H}_0^L \text{ is } \tilde{H}_0^L = \sum_{j=1}^{\frac{1}{2}(L+1)} \sum_S \eta_j (\hat{g}_{js}^\dagger \hat{g}_{js} + \hat{h}_{js}^\dagger \hat{h}_{js}) \quad (5) \quad \text{single-particle spectrum:}$$

Here \hat{g}_{js}^\dagger describes particle-like excitation: adding particle with energy $+\eta_j$.
and \hat{h}_{js}^\dagger describes hole-like excitation: removing particle with energy $-\eta_j$.



The many-body spectrum consists of combinations of these excitations:



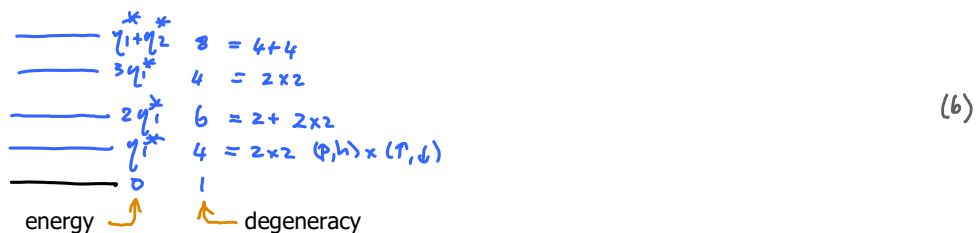
At the fixed point, each η_j takes its fixed-point value η_j^* (depicted here)

11

12

-15

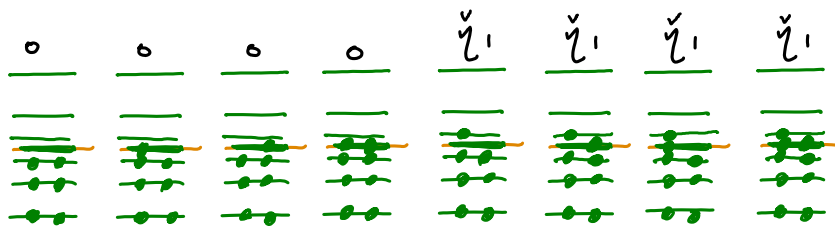
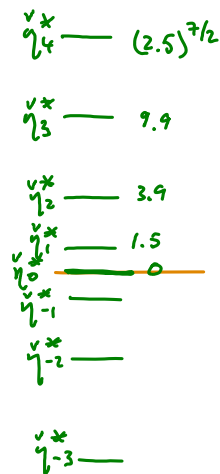
The lowest-lying excitations at fixed-point spectrum of 'even fixed point' of \mathbb{T}^2 , say $\tilde{H}_0^*, \text{even}$:



Spectrum for $d+1 = \text{odd}$

Diagonalized form of \tilde{H}_0^d is
$$\tilde{H}_0^d = \sum_s \tilde{\eta}_0 \hat{g}_{0s}^\dagger \hat{g}_{0s} + \sum_{j=1}^{\frac{1}{2}d} \sum_s \tilde{\eta}_j (\hat{g}_{js}^\dagger \hat{g}_{js} + \hat{h}_{js}^\dagger \hat{h}_{js}) \quad (7)$$

The only (but important) difference to $d+1 = \text{even}$ is the occurrence of a zero-energy level: $\tilde{\eta}_0 = 0$. All four ways of filling it (empty; spin-up; spin-down; double-occupied) yield the same energy. Hence every many-particle excitation is four-fold degenerate.



At the fixed point, each $\tilde{\eta}_j$ takes its fixed-point value $\tilde{\eta}_j^*$ (depicted here)

The lowest-lying excitations at fixed-point spectrum of 'odd fixed point' of \mathbb{T}^2 , say $\tilde{H}_0^*, \text{odd}$:



4. Kondo model: fixed points and RG flow

(no magnetic field, $h = 0$
at symmetry point, $\epsilon_d = -U/2$)

NRG-II.4

[Wilson1975, Section VIII]

$$H_{\text{Kondo}}^{\mathcal{L}} = J \hat{S}_d \cdot \hat{S}_c + H_{\text{chain}}^{\mathcal{L}} \quad (1)$$


$$\hat{S}_c = \sum_{ss'} \sum_k \hat{c}_{ks}^\dagger \frac{1}{2} \bar{\sigma}_{ss'} \cdot \sum_{k's'} \hat{c}_{k's'} = \sum_{ss'} \hat{f}_{0s}^\dagger \frac{1}{2} \bar{\sigma}_{ss'} \cdot \hat{f}_{0s} \quad (2) \quad (\text{since } \sum_k \hat{c}_{ks} = \hat{f}_{0s})$$

Rescaled Hamiltonian:
$$\tilde{H}_{\text{Kondo}}^{\mathcal{L}} = \lambda^{(\mathcal{L}-1)/2} J \hat{S}_d \cdot \hat{S}_c + \mathbb{1}_2 \otimes \tilde{H}_0^{\mathcal{L}} \quad (3)$$

The Kondo model has two fixed points, corresponding to $J = 0$ and $J = \infty$

(i) Free 'local moment' (LM) fixed point ($J = 0$)

$$\tilde{H}_{\text{Kondo}}^{\mathcal{L}}(J=0) = \text{Diagram} = \mathbb{1}_2 \otimes \tilde{H}_0^{\mathcal{L}} \quad (4)$$


Has the same spectrum as $\tilde{H}_0^{\mathcal{L}}$, with doubled degeneracy (due to two impurity states \uparrow, \downarrow)

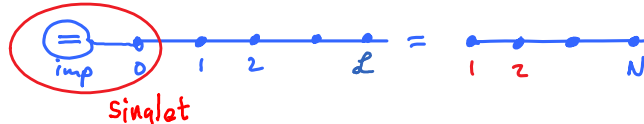
Fixed-point Hamiltonians:
$$\tilde{H}_{\text{LM, even}}^* = \mathbb{1}_2 \otimes \tilde{H}_{0, \text{even}}^* \quad \tilde{H}_{\text{LM, odd}}^* = \mathbb{1}_2 \otimes \tilde{H}_{0, \text{odd}}^*$$

For $\mathcal{L}+1 =$ $\left\{ \begin{array}{l} \text{even: (3.6) } \times 2 \quad H_{\text{LM, even}}^*: 0(2), \eta_1^*(8), 2\eta_1^*(12), 3\eta_1^*(16), \eta_2^*(16) \end{array} \right. \quad (5)$

$\left\{ \begin{array}{l} \text{odd: (3.8) } \times 2 \quad H_{\text{LM, odd}}^*: 0(8), \eta_1^*(32), 2\eta_1^*(48), \eta_2^*(32), 3\eta_1^*(32) \end{array} \right. \quad (6)$

[Eqs. from NRG-II.3]

(ii) Strong-coupling (SC) fixed point ($J = \infty$)

$$\tilde{H}_{\text{Kondo}}^{\mathcal{L}}(J=\infty) = \text{Diagram} = \tilde{H}_0^{\mathcal{L}-1}$$


To minimize effect of exchange coupling, all low-energy states have $\langle \hat{S}_d \cdot \hat{S}_c \rangle = 0 \quad (7)$

i.e. impurity and site 0 form a singlet. Thus $\langle \hat{f}_{0s}^\dagger \hat{f}_{1s} + \hat{f}_{1s}^\dagger \hat{f}_{0s} \rangle = 0$, since hopping to or from site 0 would break the singlet! Hence:

Fixed-point Hamiltonians:
$$\tilde{H}_{\text{SC, even}}^* = \tilde{H}_{0, \text{odd}}^*, \quad \tilde{H}_{\text{SC, odd}}^* = \tilde{H}_{0, \text{even}}^* \quad (8)$$

For $\mathcal{L}+1 =$ $\left\{ \begin{array}{l} \text{even: (3.8)} \quad \tilde{H}_{\text{SC, even}}^*: 0(4), \eta_1^*(16), 2\eta_1^*(24), \eta_2^*(16), 3\eta_1^*(16) \end{array} \right. \quad (9)$

$\left\{ \begin{array}{l} \text{odd: (3.6)} \quad \tilde{H}_{\text{SC, odd}}^*: 0(1), \eta_1^*(4), 2\eta_1^*(6), 3\eta_1^*(4), \eta_2^*(4) \end{array} \right. \quad (10)$

[Eqs. from NRG-II.3]

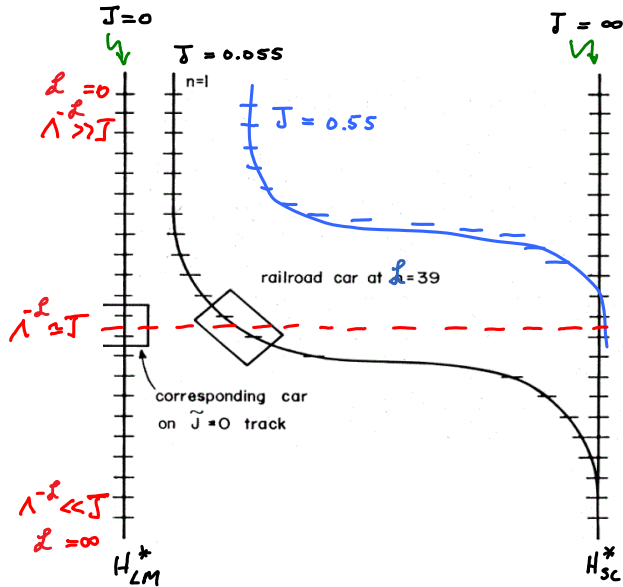
What happens for general coupling J ?

The low-energy spectrum of $\tilde{H}_{\text{Kondo}}^{\mathcal{L}} (J \ll 1)$ evolves ('flows') with \mathcal{L} , flowing from \tilde{H}_{LM}^* (even/odd) \rightarrow \tilde{H}_{sc}^* (even/odd).

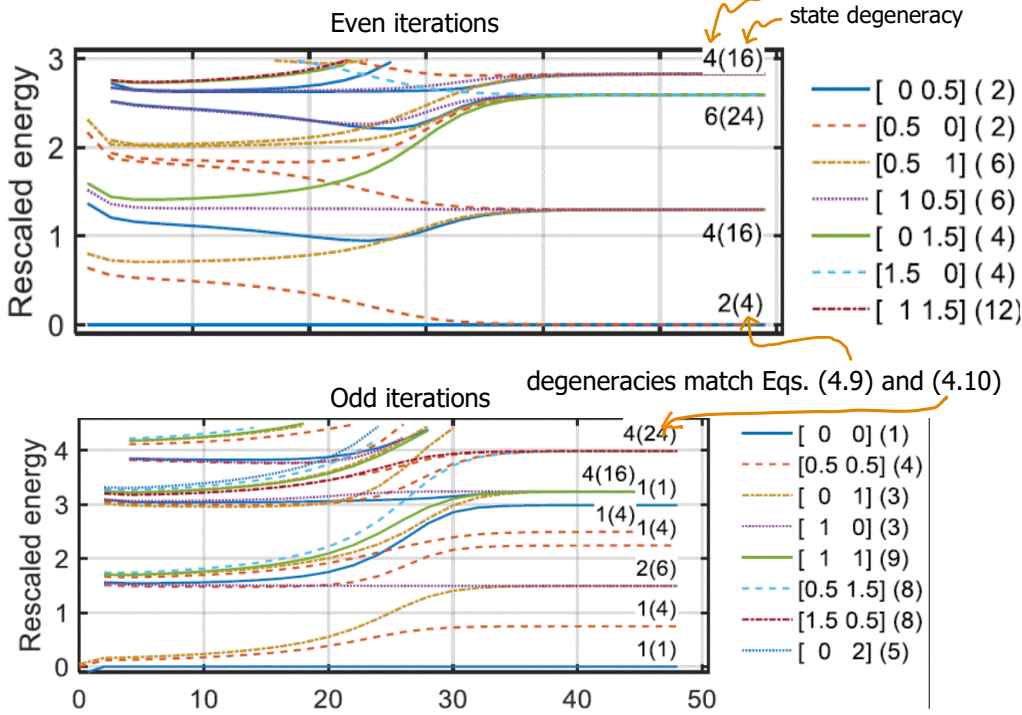
Wilson's railroad analogy [Wilson1975, p.809]

The basic results of the Kondo calculation can be summarized in a geographical allegory. The sequence of Hamiltonians corresponding to adding successive layers of the onion to the impurity will be represented by a railroad track. The length of track from the beginning to the n th tie represents the Hamiltonian containing n conduction band single electron states (that is, the n th Hamiltonian contains n particle creation and destruction operators). There is a separate railroad track for each different strength of coupling to the impurity. The approximate numerical solution of this sequence of Hamiltonians is represented by a railroad car which travels down the track. Solving the n th Hamiltonian corresponds to having the railroad car at the n th tie on the track. The set of energy levels actually computed corresponds to the length of track covered by the railroad car; as the car moves down the track (i.e., as n increases) it covers a smaller and smaller fraction of the total track up to the n th tie.

FIG. 14. Railroad track analogy for the Kondo calculation. Different tracks correspond to different initial values of \tilde{J} . A track from the top of the figure to the n th tie corresponds to the Kondo Hamiltonian with n electron states kept. The railroad cars illustrate the subset of energy levels actually kept in the numerical calculations.



Kondo model: $J = 0.11, \Lambda = 2, \text{SU}(2)_{\text{charge}} \otimes \text{SU}(2)_{\text{spin}}$ symmetry

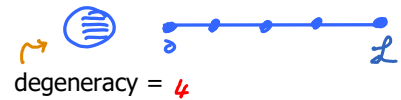


[Krishna-murthy1980a, Sec. III]

$$H_{SIAM}^{\mathcal{L}} = \sum_s \epsilon_d \hat{d}_s^\dagger \hat{d}_s + U \hat{n}_{d\uparrow} \hat{n}_{d\downarrow} + \int \frac{\Gamma}{\pi \nu} \sum_s (\hat{d}_s^\dagger \hat{f}_{0s} + h.c.) + H_{chain}^{\mathcal{L}} \quad (1)$$

Free-orbital (FO) fixed point

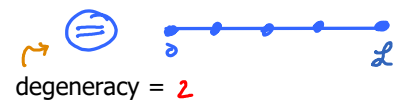
If $U = \Gamma = \epsilon_d = 0$, impurity is decoupled from bath and all four impurity states are degenerate.



Fixed-point Hamiltonians: $\tilde{H}_{FO, \text{even}}^* = \mathbb{1}_4 \otimes \tilde{H}_{0, \text{even}}^*$ $\tilde{H}_{FO, \text{odd}}^* = \mathbb{1}_4 \otimes \tilde{H}_{0, \text{odd}}^*$ (2)

Local moment (LM) fixed point

If $\epsilon_d < -\Gamma$ and $\Gamma \ll U$, impurity contains single electron behaving as a local moment, with two degenerate spin states.



Fixed-point Hamiltonians: $\tilde{H}_{LM, \text{even}}^* = \mathbb{1}_2 \otimes \tilde{H}_{0, \text{even}}^*$ $\tilde{H}_{LM, \text{odd}}^* = \mathbb{1}_2 \otimes \tilde{H}_{0, \text{odd}}^*$ (3)

Strong-coupling (SC) fixed point

For $\Gamma \rightarrow \infty$ at fixed U , site zero couple so strongly to impurity that it decouples from bath, changing its parity.



Fixed-point Hamiltonians: $\tilde{H}_{SC, \text{even}}^* = \tilde{H}_{0, \text{odd}}^*$ $\tilde{H}_{SC, \text{odd}}^* = \tilde{H}_{0, \text{even}}^*$ (4)

RG flow for $\Gamma \ll U$ (for $\mathcal{L}+1 = \text{even}$)

[Krishna-murthy1980a]

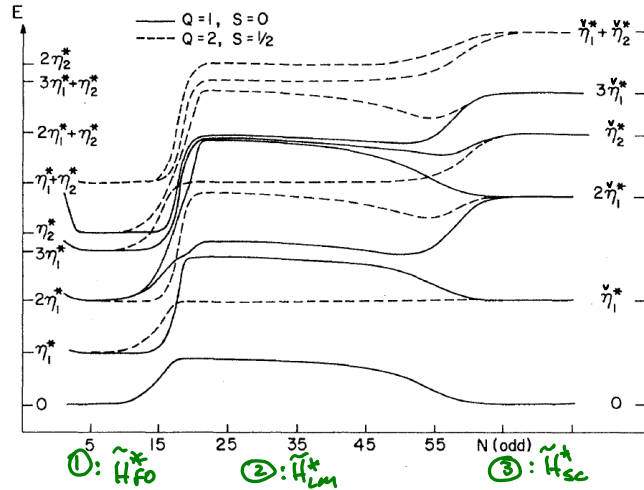
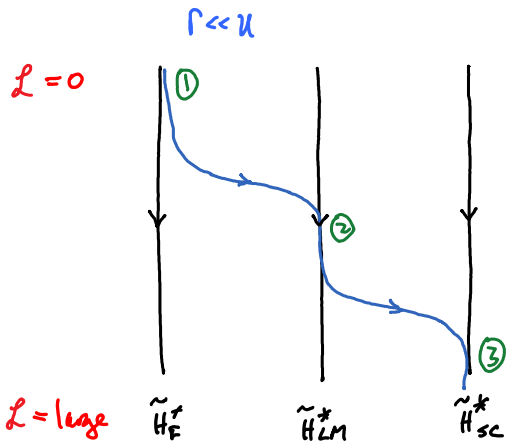


FIG. 5. Low-lying energy levels of H_N as a function of odd N for $U/D = 10^{-3}$, $U/\pi\Gamma = 12.66$, and $\Lambda = 2.5$. On the left-hand vertical scale are the lowest-lying free-orbital fixed-point levels for N odd, while on the right-hand side are the equivalent levels for N even. The following fixed-point regimes obtain: free orbital $5 < N < 15$, local moment $23 < N < 51$, strong coupling $61 < N$.

The fact that the level structures of \tilde{H}_{FO}^* , \tilde{H}_{LM}^* and \tilde{H}_{sc}^* show up as regions of near-stationarity, proves numerically that these are fixed points! Crossover from even-type η_j levels to odd-type $\check{\eta}_j$ levels proves screening, i.e. singlet-formation between impurity and site 0.

RG flow for $\Gamma \gtrsim U$ (for $\mathcal{L}+1 = \text{even}$)

[Krishna-murthy1980a]

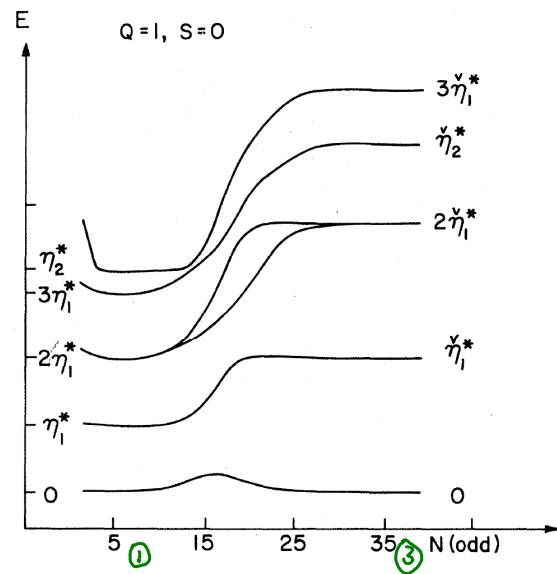
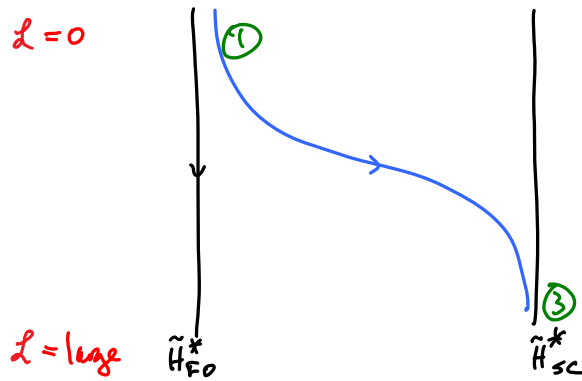


FIG. 6. Low-lying energy levels of H_N as a function of odd N for $U/D = 10^{-3}$, $U/\pi\Gamma = 1.013$, and $\Lambda = 2.5$. There is direct transition between the free-orbital and strong-coupling regimes without passing through the local-moment regime.

No local moment forms, since there is no regime where $\langle \hat{n}_d \rangle = 1$. However, if $\Gamma \rightarrow \infty$ we have $\langle \hat{d}_s^\dagger f_{0s} + h.c. \rangle = 0$, so site 0 again decouples, so flow is again toward \tilde{H}_{sc}^* , even odd.